Cancrinite synthesis from natural kaolinite by high pressure hydrothermal method: Application to the removal of Cd2+ and Pb2+ from water

Véronique Wernert, Oliver Schaef, Lobna Aloui, Carine Chassigneux, Fadhila Ayari, Dalila Ben Hassen Chehimi, Renaud Denoyel

Cancrinite synthesis from natural kaolinite by high pressure hydrothermal method: application to the removal of Cd^{2+} and Pb^{2+} from water

Véronique Wernert[1]*, Oliver Schaef[1], Lobna Aloui[1,2], Carine Chassigneux[1], Fadhila Ayari[2], Dalila Ben Hassen Chehimi[2], Renaud Denoyel[1]

[1]Aix-Marseille University, CNRS, MADIREL UMR 7246, 13397 Marseille Cedex 20, France.
[2] Laboratory of Applications of Chemistry to Natural Resources and Substances and the Environment (LACReSNE), University of Carthage, Faculty of Sciences of Bizerte, Zarzouna 7021 Bizerte, Tunisia

*corresponding author:
Véronique Wernert
Tel +33 413 551 840
Email: veronique.wernert@univ-amu.fr

Abstract

Zeolites were synthesized from natural Tunisian clay by hydrothermal treatment under high pressure (100 MPa H_2O pressure) at different gradients of temperature in high pressure autoclaves. The natural clay was first heated at 650 °C (HC-heated clay) and then transformed to an amorphous phase at 650 °C by adding different amount of NaOH. By increasing temperature and NaOH content, low-density frameworks zeolites like faujasite are transformed into more stable zeolites having higher density frameworks like cancrinite due to dissolution and recrystallisation steps. Cancrinite ($Na_8(H_20)_2CO_3[Al_6Si_6O_{24}]$) (IZA-code: CAN) was successfully synthesized with a good purity. The synthesized CAN was characterized by X-ray diffraction (XRD) and Scanning Electron Microscopy (SEM). The removal performance of heavy metal ions (Cd^{2+}, Pb^{2+}) from solution by pure CAN and clays has been studied. The kinetics of adsorption of Cd^{2+} and Pb^{2+} are very fast: equilibrium is reached within 2 minutes at 298K. The capacity of adsorption of CAN is higher for Pb^{2+} (192 mg/g) than for Cd^{2+} (68 mg/g). Adsorption equilibrium of Cd^{2+} and Pb^{2+} on CAN were well represented by Langmuir equation although the thermodynamic study reveals a more complex mechanism: thermodynamic parameters, such as equilibrium constant, free energy, entropy and enthalpy for adsorption were obtained from the experimental data, including adsorption microcalorimetry.

Keywords: high pressure hydrothermal synthesis, metakaolinite, cancrinite, heavy metals, cadmium, lead, adsorption, calorimetry,

1. Introduction

Zeolites are essentially aluminosilicate minerals with a three-dimensional open structure containing water molecules and extraframework charge compensating ions, that have attracted considerable attention due to their potential applications in many fields, such as in environmental and industrial applications. Their high cation exchange capacity, their large internal surface area, and their structural characteristics facilitate pollutant adsorption [1, 2, 3, 4, 5]. Generally, zeolites are synthesized from sodium aluminosilicate gels formed from various silica and alumina sources by hydrothermal treatment under autogeneous pressure [6]. But these precursors are relatively expensive, so several researches have been made to find other less expensive sources. For example it was shown that various types of zeolites could be produced from natural sources such as fly ash by hydrothermal reaction in alkaline solution [7, 8], kaolinite (by hydrothermal treatment [9]) or mixture kaolinite-fly ash [10] and synthesis from artificial glasses [11, 12, 13, 14]. Today clay minerals are an important source for the synthesis of zeolites because they are abundant and inexpensive. Different types of clay minerals have been used as a source of silicon and aluminium for the synthesis of zeolite, such as kaolinite [15, 16, 17, 18, 19, 20], bentonite [21] and illite [22]. Kaolinite is the most widely used phyllosilicate for the synthesis of zeolites due to its high reactivity with alkaline solutions and its total amorphization at 650 °C. In literature, two methods have been studied for synthesizing the zeolite from clay: direct hydrothermal treatment and fusion method [19, 22]. Briefly, kaolinite is first transformed into metakaolinite at high temperature (around 600 °C) in order to form reactive metakaolinite precursor. Metakaolinite is then mixed with NaOH solution and submitted to hydrothermal treatment at different temperature under autogeneous pressure for a few hours to obtain various zeolites. Reviews about the synthesis of zeolites from kaolinite are presented in references [23, 24].

In this study we propose to treat kaolinite a first time at 650°C. The obtained metakaolinite is treated a second time with NaOH at different concentrations at 650°C in order to amorphizise persisting illite and quartz and to have a more reactive amorphous phase. This sample is then treated by the high pressure (hp-) hydrothermal method. The hp-hydrothermal method uses water as the solvent and the reaction medium is in a closed system [11, 12, 13, 14]. The formation of a true solution is assumed, in which the Si and Al tetrahedral units as well as the alkali- and alkaline-earth cations with their respective hydration spheres are transported. Type and quantity of cations determine the zeolite channel diameter to be formed, because charge compensating alkali metal cations like Na^+, K^+ and Li^+ and alkaline earth metal cations such as Ca^{2+} and Ba^{2+} with their respective hydration spheres serve in general as inorganic

templates for the zeolite channel system to be formed. The method implies that different cations can template different zeolite structure types. In short, cations play the role of structure direction, framework charge balancing and pH adjustment in the synthesis of aluminosilicate zeolites.

Synthetic cancrinite like compounds were synthesized for the first time in the beginning of 1920s and from that time on, a large number of works devoted to their composition, crystallochemistry, and properties were published. CAN zeolites are synthesized from kaolinite in NaOH solution by hydrothermal synthesis in presence or absence of carbonates [25]. Without the addition of carbonates, carbonate cancrinite are also obtained due to the solubility of atmospheric CO_2 in very basic solutions [26]. Both sodalite (SOD) and cancrinite (CAN) have the common chemical formula $Na_6[Al_6Si_6O_{24}].2NaX{\cdot}6H_2O$, where X can be OH^-, Cl^-, NO_3^-, $1/2CO_3^{2-}$, or $1/2SO_4^{2-}$. However, their structural frameworks are different. CAN has a hexagonal framework that contains small ε-cages consisting of five 6-membered rings and six 4-membered rings, which give rise to large continuous channels consisting of 12-membered rings with a free dimension of ~5.9 Å. In general, these aluminosilicates are characterized by a three-dimensional framework, which contain cages and channels in their negatively charged frameworks because of the substitution of Si^{4+} ions by Al^{3+} ions. Both the β- and ε- cages need positively charged species to neutralise them. Cations can enter these porous materials to balance the charge of their structural frameworks. Structural data of these zeolite frameworks are published by the 'Structure Commission of the International Zeolite Association' (IZA). Low-silica zeolites with Si/Al≈1 such as cancrinite CAN have important industrial application because they have high cation exchange capacity (CEC). The CAN synthesized in this study was used for the removal of heavy metals like Cd^{2+} and Pb^{2+}. The presence of heavy metals in industrial effluents constitutes a major problem on human health and the environment. Cd^{2+} and Pb^{2+} are very toxic and have to be removed from wastewaters. Several methods have been developed for the removal of heavy metals from wastewater, including chemical precipitation, ion exchange, solvent extraction, reverse osmosis, and membrane filtration [27]. However, these methods have some drawbacks such as incomplete metal ion removal, high reagent and energy requirements, generation of toxic sludge and long desorption time.

Adsorption is considered as an effective and economic method for metal ion removal. Nowadays, many researches have focused on developing natural, renewable, and low-cost adsorbents, such as clays [28], and zeolites [29].

In this study, CAN zeolite was prepared from natural clay by high pressure-hydrothermal syntheses during 21 days. The influence of NaOH concentration and temperature in the formation of zeolites was studied. The kinetics and isotherms of adsorption of Cd^{2+} and Pb^{2+} on synthesized CAN and clays are determined by using the solution depletion method. The equilibrium constant of adsorption and free energy are determined by modelling the isotherm of adsorption with the Langmuir equation. The enthalpy of adsorption is obtained by calorimetry and the entropy of the process can thus be determined.

2. Experimental

2.1. Materials

The natural kaolinite clay used in this study was provided from Ghardimaou (North West of Tunisia). The clay was purified before use. To remove organic matter and impurities 0.2 mol dm^{-3} of HCl was added to the clays with a solid/liquid ratio (1:10). The mixture was stirred for 12 h until complete homogenization. The fine fraction (particle size<2 μm) was taken after stirring during 24 h for five times. The clay was then washed with distilled water until the surnageant was chloride free as confirmed by the $AgNO_3$ test. The obtained sample was dried at 80°C, milled and sieved through 63 μm mesh. The purified clay containing kaolinite is named Agh and it was used for all syntheses of CAN zeolite and for the adsorption experiments.

Other reagents used in the activation of the raw materials were: sodium hydroxide, NaOH, as pellets (obtained from Carlo ERBa reagent chemical company, purity 97%) and ultrapure water.

Heavy metal salts ($CdCl_2.2.5H_2O$ and $Pb(NO_3)_2$) used as adsorbate in this study were supplied from Aldrich.

2.1. Synthesis of CAN by the high pressure (hp)-hydrothermal method

2.2.1. Alkaline fusion of the natural clay in presence of CO_2

A conventional alkaline fusion method was used for the synthesis of zeolite from purified clay (Agh). Approximately 1g of kaolinite was heated at 650°C for 2 hours in a furnace under air. This amorphous solid (heated clay, HC) was then mixed with 25 ml of NaOH solutions with various concentrations in order to obtain different NaOH/HC ratios (0.66, 1 and 4). The gel was dried at 100 °C during 24 hours and calcined again at 650°C. The obtained powder was cooled, ground and subsequently used as precursor for high pressure hydrothermal synthesis of zeolites. The influence of carbonates on the formation of the zeolites was studied. To avoid formation of carbonates the calcination of the clay sample was carried out in a furnace under Ar in an oven at 650 °C. This powder was then mixed with NaOH (NaOH/HC=0.66 and 4 mass ratio). The gel was dried at 100°C during 24 hours under Ar and then calcined in a furnace under Ar in an oven at 650 ° C for 2 hours. The powders obtained were cooled and ground.

2.2.2 High pressure hydrothermal synthesis

The zeolites were synthesized by hydrothermal treatment of these powders prepared by two different methods in presence and in absence of atmospheric CO_2 under 100 MPa water pressure at different temperatures. The hydrothermal synthesis is described in detail by Ghobarkar *et al.* [14]. Briefly, the powders were placed in four Teflon containers, which were completely filled up with distilled water (volume ratio powder/water = 1/3). The Teflon containers were placed in a high pressure autoclave (Autoclave Engineers, USA), closed and placed in a vertical furnace. The experiments were conducted isothermally, but in a temperature gradient, between 40 and 305°C depending on the furnace temperature chosen. The temperature in the four containers increases from the bottom to the top. The four containers are named very low (VL), low (L), medium (M) and high (H) temperatures. In each container there is a gradient of temperature which is known by calibration. The gradient of temperature for each container is indicated in the figure captions (see figures 2 and 3). Once the desired furnace temperature was achieved, the external water pressure was applied using a Sitec (Switzerland) manual hydraulic piston pump by which distilled water was pumped into the autoclave until 100MPa water pressure was obtained. The hydrothermal synthesis is running for 21 days. The hydrothermal synthesis at high pressure takes relatively long time. However, during application, the obtained products are more stable against subsequent dissolution in aqueous solutions (in comparable pH ranges) than zeolite products obtained under low pressure (autogeneous) synthesis conditions. This is due to the absence of mayor defects during the synthesis process as the crystallization passes by a "true" dissolution-recrystallisation process excluding transport and integration of colloidal units as in the case of classical zeolite synthesis at low pressure [30].
For the adsorption experiments several grams of CAN have to be synthesized by using larger containers, while the preliminary study was used to determine the experimental conditions. After synthesis, the CAN was washed with ultrapure water before adsorption experiments until the pH of the rinsing water was stable around pH 6.

2.3. Characterization of the starting material and as synthesized zeolites

The samples were characterized by a variety of conventional techniques. Mineralogical analysis of the raw sample was carried out by X-ray diffraction (Bruker, Germany, D-5000

diffractometer). Data collection was carried out in the 2θ range 2-60° (Cu K_α). Phase identification was performed by searching the ICDD powder diffraction file database, with the help of Joint Committee on Powder Diffraction Standards (JCPDS) files. The morphology was characterized by a scanning electron microscope (SEM, Philips SEM XL30Sfeg FEI, The Netherlands).

2.4 Adsorption kinetics

The kinetics of adsorption of Cd^{2+} and Pb^{2+} on clays and CAN were determined at 298K. 50 mg of CAN zeolite were added to 20 cm^3 of aqueous solutions containing Pb^{2+} or Cd^{2+} at the concentrations of 0.5 mmol dm^{-3} and 1 mmol dm^{-3}, respectively. Those solutions were prepared from 0.1 mol dm^{-3} of $CdCl_2.2.5H_2O$ and $Pb(NO_3)_2$ stock solutions. The solutions were mixed at 298K during different times varying between 1 minute and 2 hours. The separation of the liquid and solid phase was carried out by filtration by using nylon filters and the cations were then analyzed by atomic absorption spectroscopy. Blank experiments were also conducted without zeolites in order to verify that the metallic cations were not adsorbed on the nylon filters. The concentrations of Cd^{2+} and Pb^{2+} in the solution were determined by atomic absorption spectroscopy (SpectrAA 600 électrothermique, Agilent Technologies). The amount of Cd^{2+} and Pb^{2+} adsorbed at each time t, q_t (mg g^{-1}), was calculated by using equation 1:

$$q_t = \frac{(C_0 - C_t).V}{m} \quad (1)$$

where, C_0 is the initial metal ion concentration (mg dm^{-3}); C_t is the metal ion concentration measured at time t (mg dm^{-3}); V is the volume of the solution (dm^3) and m is the amount of the adsorbent (g).

2.5. Adsorption isotherms

The adsorption isotherms of Cd^{2+} and Pb^{2+} were determined by the solution depletion method at 25°C. Each solution was diluted from a stock solution in order to have solutions of different

concentrations. Glass bottles containing 25 mg of adsorbent and 10 cm^3 of solution were sealed and shaken automatically for 24 hours at 298K. The initial pH of the solution was around 6. The pH was controlled after adsorption in order to verify that there is no precipitation of heavy metals. After equilibrium, the suspensions were centrifuged and the concentrations of Cd^{2+} and Pb^{2+} in the solution were determined by atomic absorption spectroscopy.

The amount of Cd^{2+} and Pb^{2+} adsorbed at equilibrium, q_e (mg g^{-1}), was calculated by using equation 1 at equilibrium ($q_e = \frac{(C_0 - C_e).V}{m}$), where C_e is the metal ion concentration at equilibrium (mg dm^{-3}).

2.6 Calorimetry

To measure the energy of interactions between the adsorbent (clay, zeolites) and heavy metals (Pb^{2+}, Cd^{2+}) we used a Tian-Calvet type microcalorimeter of TA instruments (TAM III model) [31]. A stock solution of the heavy metal was injected step by step inside the microcalorimetric cell, in which the solid is put in suspension in water thanks to a propeller. At each step, the measured heat has a contribution of both dilution and sorption phenomena [32]. The dilution contribution was measured by the same procedure but without the solid inside the cell. It was subtracted from the measured heat to get the sorption enthalpy. The integral sorption enthalpy was obtained by dividing the cumulative heat by the total sorbed amount. The adsorption experiments were done at 298K.

3. Results and discussion

3.1. Synthesis of CAN

3.1.1 Effect of the NaOH/HC ratio

Clay is calcined a first time at 650°C under air. Heated clay is then treated at 650 °C under air with different concentrations of NaOH (NaOH/HC=0.66, 1 and 4) prior to the hp-hydrothermal synthesis. The temperature and the concentration of NaOH in this second calcination strongly influence the zeolites obtained under hp-hydrothermal treatment for 21 days. Similar experiments were done under Ar in order to avoid the formation of carbonates and to study the influence of carbonates on the formation of CAN. In a first step the experiments were done in small containers in order to better understand the influence of several parameters such as NaOH/HC ratios, presence of carbonates and temperature on the zeolites obtained. In a second step the zeolites are synthesized in larger containers in order to have enough zeolite to perform the adsorption and calorimetric studies. After hp-synthesis the products were dried and analysed by XRD.

First, the results obtained in small containers are presented. The products obtained after hp-hydrothermal synthesis at different temperatures and for various NaOH/HC ratios are given in Table I. For low NaOH/HC=0.66 under air a mixture of zeolites among them faujasite (FAU) and gismondine (GIS) was obtained. FAU and GIS have only water molecules and cations, but no anions in the pores. Under Ar a mixture of chabazite (CHA), natrolite (NAT), GIS and analcime (ANA) was obtained. Tectosilicate phases like nepheline and quartz are also present. Nepheline and quartz have a high-density framework and are thus thermodynamically stable [14]. Nepheline has no water in the structure. Those phases could be obtained during the calcination step at 650°C in presence of NaOH or obtained after hp-hydrothermal treatment. Quartz is present in the clay used for this study. For NaOH/HC=1, under air, a mixture of FAU, GIS, ANA, CAN and SOD was obtained for temperature ranging between 55 and 170°C. Nepheline and quartz were still present. SOD and CAN zeolites have anions (OH^-, CO_3^{2-}) in their pores and were generally obtained in NaOH rich solutions and at high temperature [33, 34]. CAN and SOD have the same chemical composition but different frameworks: cubic for SOD and hexagonal for CAN as explained in the introduction. ANA formula is $Na_2AlSi_2O_6.H_2O$ and has no anions in his structure. Gualtieri (2001) [35] propose that FAU and GIS co-crystallise at low temperature (90°C) and at higher temperature (150°C) FAU dissolves before GIS, which in turns transforms into ANA. Some authors propose the phase transformation from SOD to CAN [33]. In our study all the experiments are made during 21 days and the phase transformation cannot be observed. We observe co-

crystallisation of the different phases. For higher temperature (170-295°C), ANA, CAN, GIS and traces of SOD were obtained. By increasing the NaOH/HC ratio to 4, under air, thermonatrite ($Na_2CO_3.H_2O$) and CAN were obtained for temperatures lower than 160°C whereas for temperature higher than 160°C pure CAN was obtained. The increase of temperature and NaOH leads to the formation of CAN which has a higher framework density than the other zeolites obtained like FAU, CHA, NAT and is thus more stable. In fact, most of the open microporous structures are metastable thermodynamically, so, many zeolites can transform to more stable structures under heating [36]. For open structures OH^- can enter in the channel of the zeolite, interact with the cation and thus destabilize the structure and dissolve the zeolite. The zeolite is completely dissolved and crystallizes in a more stable zeolite having a higher density framework. In fact, the density framework of FAU is 13 T-atoms/nm^3 and the density framework of CAN is 16.5 T-atoms/ nm^3. This study shows the transformation of low density framework zeolites like FAU, CHA and NAT into more thermodynamically stable density framework zeolites like CAN, ANA or GIS by a process of dissolution and recrystallisation by increasing temperature and NaOH content. The rate of dissolution of FAU, CHA and NAT increases with OH^- or temperature and the growth rate of CAN, ANA and GIS too.

3.1.2. Synthesis of CAN for NaOH/HC=4 in small containers

The synthesis of CAN is presented in more detailed in this part for NaOH/HC=4. The XRD patterns of the starting materials that means purified clay (Agh), heated clay at 650°C (HC) and heated at 650°C with NaOH/HC=4 in presence of CO_2 are shown in figure 1. Kaolinite (K) phase in the purified clay (Agh) before calcination (figure 1a) is identified by its XRD characteristic peaks at 12° and 25° 2θ. Illite (Ill) and quartz (Qz) are also present. After treatment of Agh at 650°C (figure 1b) the peak of kaolinite disappears due to its transformation into metakaolinite but the quartz and illite phases are still present. Metakaolinite is amorphous and the highest diffraction peaks correspond to the presence of quartz (SiO_2) and illite. The illite phase has completely disappeared after activation of heated clay (HC) with NaOH (NaOH/HC=4) in presence of CO_2 at T=650°C but quartz is still present. Sodium carbonate (Na_2CO_3) appears after the treatment with high concentrations of NaOH (figure 1c). In presence of atmospheric CO_2 and alkaline solution, carbonates are formed. Figure 2 shows the XRD patterns of the products synthesized at four ranges of temperatures: 100-160°C (VL) 160-225°C (L) 225-275°C (M) and 275-305°C (H) under air

for NaOH/HC=4. The diffractograms of samples prepared at 100-160°C (VL) show that all XRD peaks agree well with the characteristics peaks of phase mixtures of cancrinite zeolite (CAN) and thermonatrite ($Na_2CO_3.H_2O$) but at higher temperatures 160-305°C only CAN was formed. Thermonatrite (Na_2CO_3, H_2O) is obtained from the sodium carbonate present in the precursor as shown in figure 1c. By increasing the temperature in the range of 160 and 305°C pure cancrinite was obtained. The disappearance of the thermonatrite phase at higher temperature is explained by its reaction with the amorphous phase to give CAN. The SEM micrographs reveal that clay samples contain agglomerates with some irregularities in size and morphology (figure 3a). After addition of NaOH to metakaolinite (NaOH/HC = 4) and recalcination at 650°C under air one can see the formation of microspheres with high agglomeration which have relatively uniform particle sizes (figure 3b). The typical SEM image of the morphology for zeolites obtained after hydrothermal treatment are exhibited in figure 3c, where a typical hexagonal cancrinite morphology is observed. The highly symmetric hexagonal needle or stick shape reflected cancrinite hexagonal symmetry (P6) is an indication of high crystallinity. The syntheses are reproducible and verified at least three times. For NaOH/HC=4, under Ar, a mixture of CAN, GIS and ANA was obtained in the range of temperature studied (160-305°C). It has been shown previously that the presence of carbonates stabilizes the formation of CAN by entering in the broad channel of the structure [37]. To summarize CAN was obtained for NaOH/HC=1 but the purity was limited in the small containers due to the large gradient of temperature leading to the formation of several zeolite phases due to the dissolution and recrystallization processes.
Experiments were done in larger containers having smaller gradients of temperature.

3.1.2. Synthesis of CAN NaOH/HC=1.2 in large containers

The compounds obtained in large containers are given in table II. The products obtained show that the size of the container influences the type of zeolite obtained. This could be explained by the gradient of temperature which is smaller in the larger containers. ANA was obtained for NaOH/HC=0.66 and CAN with traces of thermonatrite were obtained for NaOH/HC=1.2 in the range of temperature studied (130-160°C). Figure 4 gives the XRD pattern of CAN synthesized zeolite in the larger containers. The SEM image of the CAN is given in figure 5. Well crystallized CAN are obtained. The CAN synthesized in large quantities is used for the adsorption experiments.

3.2 Kinetics and isotherms of adsorption of metallic cations on CAN zeolites

The adsorption experiments were performed without buffer. The control of the pH during adsorption experiments for hydrolysable metal cations has to be performed in order to avoid the hydrolysis of the cations and the precipitation. The initial pH of the solution is around 6. According to the diagram of speciation of the cations in solution, the pH of precipitation is 8 for Cd^{2+} and 7-8 for Pb^{2+}. The pH measured after adsorption experiments are below 7 for all experiments.

Figure 6 shows the effect of contact time on the adsorption capacity of Cd^{2+} and Pb^{2+} onto synthesized CAN zeolite. The kinetics of adsorption are very fast, equilibrium being reached within 2 minutes. The equilibrium concentration is very low around 10-20 μmol L^{-1}. This could be explained by the fast transport of the metallic cations to the vacant sites of the zeolite and a fast cationic exchange with the cations present in the zeolite framework. Similar results have been obtained by Mekkawi *et al.* (2014) [38] who studied the kinetic of adsorption of Pb^{2+} on zeolite Y. Simulations and NMR verifications of ion conduction in SOD and CAN by Jordan *et al.* [39] have clearly shown that the presence of anionic entities in the channel system considerably diminishes the activation energy for cation transport in both cases.

The isotherms of adsorption of Cd^{2+} and Pb^{2+} on clays (named Agh) and CAN are given in figures 7a and 7b respectively. For both cations the capacity of adsorption is higher for zeolites compared to clays. There is a strong affinity between the cations and the adsorbents. These cations moved through the pores of clays and zeolites and replace the exchangeable cations.

The isotherm can be described by the Langmuir adsorption isotherm given by eq. 2:

$$q_e = \frac{q_m K_L C_e}{1+K_L C_e} \qquad (2)$$

where q_e (mg g^{-1}) is the amount of cations adsorbed per unit weight of adsorbents, C_e (mol L^{-1}) is the equilibrium concentration, q_m and K_L are the Langmuir constants related to capacity and energy of adsorption, respectively. K_L is calculated from the activity and is thus without unity. C_e has thus to be taken in mol L^{-1} because the reference concentration is 1 mol L^{-1} [40]. The results are given in table III. The capacities of adsorption are higher on synthesized CAN than on clays. Hexaaqua complexes are formed with Cd^{2+} and Pb^{2+}. It is known that water is attracted to the positively charged cations due to its dipolar nature and the water molecules create a shell around the cation when the hydrated cation are formed. As seen from table III, a

higher capacity of adsorption is found for Pb^{2+} than for Cd^{2+} for all adsorbents. These results are in good agreement with the Coulomb law, the exchange affinity increases with the valence of the ion and with equal charge, the cation having the smallest hydrated radius is preferentially adsorbed. This confirms the order of selectivity between Pb^{2+} and Cd^{2+} (hydrated radius of Pb^{2+} (0.401 nm) <hydrated radius of Cd^{2+} (0.426 nm)).

The theoretical CEC gives the maximum capacity of an ion exchanger to accommodate foreign cations. The value can be determined from the composition of the zeolite. For carbonate cancrinite having the composition $Na_8(H_2O)_2CO_3(Al_6Si_6O_{24})$ the theoretical CEC is 805 meq/100g. The experimental CEC can be determined with NH_4^+ but the values obtained are generally lower than the theoretical CEC due to the fact that some cations located in small cages are not exchanged by NH_4^+. Those cations could be exchanged in favorable conditions such as higher temperature or smaller cations. Carbonate cancrinite has a high CEC compared to other zeolites. By considering that one divalent cation is exchanged with two Na^+ the maximum of cations adsorbed can be estimated from the CEC. The maximum capacity of adsorption for CAN could be estimated around 451 mg g^{-1} for Cd^{2+} and 833 mg g^{-1} for Pb^{2+}. The maximum of adsorption obtained experimentally for CAN is 68.4 mg g^{-1} for Cd^{2+} and 192.6 mg g^{-1} for Pb^{2+}. It has to be noted that the mass of solid is not pure CAN because an amorphous phase could be present after the synthesis. SEM images and XRD results, however, indicate that the quantities of impurities above 130°C synthesis temperature do not exceed 10vol% and consist mainly of unreacted precursor material. The amount of cations adsorbed is comparable or higher than the amount adsorbed on other types of zeolites having a higher Si/Al ratio compared to CAN which has a Si/Al ratio about 1.5. The amount of Cd^{2+} and Pb^{2+} adsorbed are respectively 52.0 mg g^{-1} and 126.2 mg g^{-1} on a mordenite zeolite having a Si/Al ratio about 7.5 [41], 9.8 mg g^{-1} and 44.3 mg g^{-1} on a mordenite having a Si/Al ratio about 9 [42], 2.9 mg g^{-1} and 34.6 mg g^{-1} on a ferrierite zeolite (Si/Al ratio 10) [41] and 7.5 mg g^{-1} and 29.7 mg g^{-1} on a ZSM-5 zeolite (Si/Al ratio 29) [42]. Higher adsorption capacities are obtained with faujasite which has a Si/Al ratio slightly comparable to CAN. The capacity of adsorption of Pb^{2+} on FAU (Si/Al ratio 2.0) is around 350 mg g^{-1}, value close to the theoretical stoichiometric cation exchange value [43]. Lower values are obtained with a zeolite X (Si/Al ratio around 1 and 1.5), the amount of Cd^{2+} adsorbed is 67 mg g^{-1} on a zeolite X [44]. The difference of adsorption capacity of metals on zeolites having comparable Si/Al ratio depends on other parameters such as the accessibility of the exchangeable cations as explained below. The ratio between experimental q_m and theoretical q_m is 0.15 for Cd^{2+} and

0.23 for Pb^{2+}. A better exchange is obtained with Pb^{2+} which could be explained by the smaller size of this cation compared to Cd^{2+}. The structure of cancrinite belongs to hexagonal space group $P6_3$ and has two kinds of micropores formed by an ordered Si and Al framework. One is a 12-membered ring channel with a diameter of 5.9 Å, and the other is a 6-membered ring channel consisting of undecahedral cages, called cancrinite cages, around the three-fold axis. One cation site Na1 is in the cancrinite cage and another cation site Na2 is in the 12-membered ring channel. There are 8 Na^+ in the cancrinite structure, 2 are in the cages and 6 are in the open channel [26]. Anions such as CO_3^{2-} or OH^- are in the center of the 12-membered ring channel. There exists one water molecule in each cancrinite cage [26]. Water could also be present in the channels, but those water molecules do not behave as zeolithic water. Miyake *et al* 2004 [45] suggest by using the Rietveld method based on the observed XRD intensities that Na^+ ions located in the cancrinite cage are not exchangeable with Pb^{2+} ions. In our case due to the low exchange only the Na^+ ions located in the 12-membered are probably exchanged with Pb^{2+} or Cd^{2+}. The pore size (5.9 Å) of cancrinite is slightly smaller than the size of hydrated cations having a hydrated diameter around 8 Å. Thus, some water molecules involved in the metal hydration have to be removed in order to accommodate the metal ions within the zeolite channel which could hinder the ion exchange process.

The data obtained by sorption experiments at 298 K were used for the determination of thermodynamic parameters: the Gibbs free energy (ΔG°), the entropy change (ΔS°), and enthalpy change (ΔH°) were calculated.

The standard free energy of adsorption is calculated by eq. 3:

$$\Delta_{ads}g^0 = -RTln(K_L) \quad (3)$$

where R is universal gas constant (8.314 $J \cdot mol^{-1} \cdot K^{-1}$), T is temperature (K) and K_L is the equilibrium constant of adsorption obtained from the Langmuir model.

The entropy of adsorption was calculated form eq. 4:

$$\Delta_{ads}s^0 = \frac{\Delta_{dpl}h - \Delta_{ads}g^0}{T} \quad (4)$$

The thermodynamic results are reported in table III. The enthalpy values are taken in the pseudoplateau adsorption region. The negative values of $\Delta_{ads}g°$ indicate that the adsorption of Pb(II) and Cd(II) on the various adsorbents occurs spontaneously. The positive values of

$T\Delta_{ads}s°$ shows that the adsorption of Cd^{2+} and Pb^{2+} is entropically favourable in agreement with calorimetry results presented hereafter. This could be explained by the fact that two Na^{+} are exchanged with one divalent cation.

3.3. Calorimetric Study.

Titration microcalorimetry allows the measurement of molar enthalpy effects accompanying ion adsorption. The enthalpy measured is due to the adsorption of the cation into the zeolites which is called in many calorimetric studies displacement. In fact, during the adsorption process there is a displacement of cations and water molecules through ionic exchange of cations and wetting/dewetting effects. The molar enthalpy of adsorption $\Delta_{ads}h$ is calculated from $\Delta_{ads}H$ and the corresponding quantity of cations adsorbed taken from the adsorption isotherm obtained in the same experimental conditions.

Figure 8 represents the evolution of the molar enthalpy of adsorption ($\Delta_{ads}h$ in kJ mol^{-1}) of Cd^{2+} on Agh and CAN and of Pb^{2+} on CAN. For kaolinite (Agh) the enthalpy for Cd^{2+} is slightly endothermal. For cancrinite the integral enthalpy of adsorption due to the cation adsorption was positive in the whole concentration range, showing clearly that the process is endothermic in the whole adsorption range. The enthalpy varies with amount adsorbed showing that not all sites have the same adsorption energy, which also indicate that the Langmuir equation cannot be applied rigorously. The observed enthalpy is due to the interaction between the cations and the zeolite and the dehydration/rehydration of the cations during the cationic exchange. Generally the adsorption process is negative (exothermic contribution in the case of a simple adsorption mechanism) whereas the dehydration is positive (endothermic contribution) since the hydration enthalpies are usually negative. The cations Cd^{2+} and Pb^{2+} could be dehydrated during the cationic exchange in order to accommodate in the zeolites and the Na^{+} ions exchanged with Pb^{2+} or Cd^{2+} are rehydrated in the solution. In fact, the size of the hydrated cations around 8 Å is higher than the pore size of the cancrinite zeolite (5.9 Å). The cationic exchange could be written:

$$2Na_Z+Me^{2+}=2Na^{+}+Me_Z$$

where Me^{2+} is the metallic cation and Na_Z and Me_Z are the cations adsorbed on the zeolites.

The enthalpy of adsorption could be estimated by knowing the binding energy between the cations (Na^{+} and Me^{2+}) and the zeolite and the hydration/dehydration of the cations (Na^{+} is rehydrated and Me^{2+} is dehydrated).

The enthalpy of adsorption could be written:

$$\Delta_{ads}h = (\Delta_{bind}h_{MeZ} - 2\Delta_{bind}h_{NaZ}) + (2\Delta_{hydr}h_{Na+} - \Delta_{hydr}h_{Me2+})$$

where $\Delta_{bind}h_{MeZ}$ is the binding energy between the metallic cation and the zeolite (Me could interact with more than one oxygen in the zeolite), there could be dehydration before the entrance in the zeolite or during the adsorption process when the cation is adsorbed on the zeolite, $-\Delta_{bind}h_{NaZ}$ *is the* desorption of Na^+ due to the cationic exchange, Na^+ is probably rehydrated in the solution and the enthalpic effect is given by $\Delta_{hydr}h_{Na+}$. To evaluate correctly the enthalpy of adsorption numerical simulation is needed. However, the difference between the two cations can be explained by higher energy of hydration for Cd^{2+} (-1806 kJ mol^{-1}) than for Pb^{2+} (-1480 kJ mol^{-1}) because the other terms in the calculation of the enthalpy of adsorption are probably comparable for both cations. Thugsuz *et al.* [46] determine by DFT the energy of binding of Cd^{2+} and Pb^{2+} on zeolite ZSM and show that those cations are linked to 4 oxygen in the zeolite framework and the binding energy is smaller for Pb^{2+} than for Cd^{2+}. The binding energy of Na and the zeolite ($\Delta_{bind}h_{NaZ}$) and the hydration enthalpy of Na^+ ($\Delta_{hydr}h_{Na+}$) are probably comparable for both cations by assuming that the Na located in the channels are exchanged in both cases.

4. Conclusions

In this work CAN zeolite was synthesized from natural clay by hp-hydrothermal synthesis with a good purity. We obtain a well crystallized hexagonal crystal of cancrinite, with Si/Al≈1.5. It was shown that zeolites having a medium density framework like CAN were obtained by increasing the NaOH content and temperature. The kinetics of adsorption of Pb^{2+} and Cd^{2+} are very fast, equilibrium being reached within one minute. The isotherms of adsorption are modeled with the Langmuir equation. The calorimetric study indicates that the cationic exchange between the metallic cations and the zeolites is endothermic and is probably due to hydration and dehydration processes. The adsorption is driven by entropy.

Acknowledgements

The authors thank Gregory Escoffier for the help in the heavy metals analysis.

References

[1] C.A. Ríos, C.D. Williams, C.L. Roberts, J. Hazard. Mater. 156 (2008) 23-35. https://doi.org/10.1016/j.jhazmat.2007.11.123

[2] A. Alshameri, C. Yan, Y. Al-Ani, A.S. Dawood, A. Ibrahim, C. Zhou, H. Wang, J. Taiwan Instit. Chem. Eng. 45 (2013) 554-564, https://doi.org/10.1016/j.jtice.2013.05.008

[3] Y. Zhao, B. Zhang, , X. Zhang, J. Wang, J. Liu, R. Chen, J. Hazard. Mater. 178 (2010) 658–664, https://doi.org/10.1016/j.jhazmat.2010.01.136

[4] N. Hamdi, E. Srasra, J. Environ. Sci., 24 (2012) 617–623, https://doi.org/10.1016/S1001-0742(11)60791-2

[5] V. Wernert, O. Schaef, H. Ghobarkar, R. Denoyel, Mic. Mes. Mat., 83 (2005) 101–113, https://doi.org/10.1016/j.micromeso.2005.03.018

[6] Q. Liu, H. Xu, A. Navrotsky, Mic. Mes. Mat. 87 (2005) 146–152, https://doi.org/10.1016/j.micromeso.2005.08.008

[7] D. Mainganye , T. Victor Ojumu , L. Petrik, Materials 6 (2013) 2074-2089, doi: 10.3390/ma6052074

[8] A.M. Cardoso, M.B. Horn, L.S. Ferret, C.M.N. Azavedo, M. Pires, J. Hazard. Mat. 287 (2015) 69-77. DOI: 10.1016/j.jhazmat.2015.01.042

[9] L. Ayele, J. Perez-Pariente, Y. Chebude, I. Dias, Mic. Mes. Mat. 215 (2015) 29-36, https://doi.org/10.1016/j.micromeso.2015.05.022

[10] C. Belviso, C. L.C. Giannossa, F.J. Huertas, A. Lettino, A. Mangone, S. Fiore, Mic. Mes. Mat. 212 (2015) 35–47, https://doi.org/10.1016/j.micromeso.2015.03.012

[11] H.Ghobarkar, Kristall und Technik 17, 459-464 (1982)

[12] H. Ghobarkar, O. Schaef, Cryst. Res. Technol. 28 (1993) 855-859, DOI: 10.1002/crat.2170280614

[13] J. Rogez, P. Knauth, A. Garnier, H. Ghobarkar, O. Schaef, J. Non-Cryst. Solids 262 (2000) 177-182

[14] H. Ghobarkar, O. Schäf, Y. Massiani, P. Knauth. The reconstruction of natural zeolites. Kluwer, Dortrecht, Boston, London 2003, DOI 10.1007/978-1-4419-9142-3

[15] A. Hadi Abdullah, N. Zulkefli, A. Shah Abd Aziz, R. Mat. Indian J. Sci. Technol. 9 (2016) . DOI: http://dx.doi.org/10.17485/ijst%2F2016%2Fv9i9%2F88726

[16] P. Asawaworarit, N. Chollacoop, N. Viriya-Empikul, A. Eiad-Ua, Mater. Sci. Forum 872 (2016) 206–210

[17] L. Ayele, J. Pérez-Pariente, Y. Chebude, I. Díaz, Appl. Clay Sci. 132-133 (2016) 485–490, https://doi.org/10.1016/j.clay.2016.07.019

[18] O.A. Ajayi, S.S. Adefila, M.T. Ityokumbul, Ain Shams Eng. J. 9 (2018) 1653-1661. DOI: 10.1016/j.asej.2016.10.008

[19] C. A. Rios, C. D. Williams, M. A. Fullen, Appl. Clay Sci. 42 (2009) 446–454, https://doi.org/10.1016/j.clay.2008.05.006

[20] A. Kongnoo, S. Tontisirin, P. Worathanakul, C. Phalakornkule, Fuel 193 (2017) 385–394, https://doi.org/10.1016/j.fuel.2016.12.087

[21] H. Ma, Q. Yao, Y. Fu, C. Ma, X. Dong, Ind. Eng. Chem. Res. 49 (2010) 454–458, https://doi-org.lama.univ-amu.fr/10.1021/ie901205y

[22] M. Mezni, A. Hamzaoui, N. Hamdi, E. Srasra, Appl. Clay Sci. 52 (2011) 209–218, http://dx.doi.org/10.1016/j.clay.2011.02.017

[23] E.B.G. Johnson, S. E. Arshad, Appl. Clay Sci. 97–98 (2014) 215–221, https://doi.org/10.1016/j.clay.2014.06.005

[24] T. Abdullahi Z. Harun M. Hafiz Dzarfan Othman, Adv. Powder Technol. 28 (2017) 1827–1840, https://doi.org/10.1016/j.apt.2017.04.028

[25] J.-C. Buhl, C. Taake, F. Stief, M. Fechtelkord, React. Kinet. Catal Lett, 69 (2000) 15-21, https://doi-org.lama.univ-amu.fr/10.1023/A:1005676322206

[26] Q. Liu, A. Navrotsky, C. F. Jove-Colon, F. Bonhomme, Mic. Mes. Mat. 98 (2007) 227–233, https://doi.org/10.1016/j.micromeso.2006.09.008

[27] R.R. Navarro, S. Wada, K. Tatsumi, J. Hazard.Mater. 123 (2005) 203–209. https://doi.org/10.1016/j.jhazmat.2005.03.048

[28] C. Grader, J.-C. Buhl, Mic. Mes. Mat. 171 (2013) 110-117, https://doi.org/10.1016/j.micromeso.2012.12.023

[29] T.C. Nguyen, P. Loganathan, T.V. Nguyen, S. Vigneswaran, J. Kandasamy, R. Naidu, Chem. Eng. J. 270 (2015) 393-404, https://doi.org/10.1016/j.cej.2015.02.047

[30] D. Berge-Lefranc, C. Vagner, R. Calaf, H. Pizzala, R. Denoyel, P. Brunet, H. Ghobarkar, O. Schaef, Mic. Mes. Mat. 153 (2012) 288–293. doi:10.1016/j.micromeso.2011.11.024.

[31] R. Denoyel, F. Giordano, J. Rouquerol, Colloids Surf. Physicochem. Eng. Asp. 76 (1993) 141–148, https://doi.org/10.1016/0927-7757(93)80072-M

[32] R. Denoyel, F. Rouquerol, J. Rouquerol, J. Colloid Interface Sci. 136 (1990) 375–384, https://doi.org/10.1016/0021-9797(90)90384-Z

[33] D.-C. Lin, X.-W. Xu, F. Zuo, Y.-C. Long, Mic. Mes. Mat. 70 (2004) 63–70, https://doi.org/10.1016/j.micromeso.2004.03.003

[34] M. Park, C. L. Choi, W. T. Lim, M. C. Kim, J. Choi, N. Ho Heo, Mic. Mes. Mat. 37 (2000) 81–89, https://doi.org/10.1016/S1387-1811(99)00196-1

[35] A.F Gualtieri, Phys. Chem. Min. 28 (2001) 719-728, https://doi-org.lama.univ-amu.fr/10.1007/s002690100197

[36] R. Xu, W. Pang, J. Yu, Q. Huo, J. Chen, Chemistry of Zeolites and Related Porous Materials: Synthesis and Structure, Ed. John Wiley and Sons, 2007, DOI:10.1002/9780470822371

[37] N. V. Chukanov, V. V. Nedelko, L. N. Blinova, L. A. Korshunova, L. V. Olysych, I. S. Lykova, I. V. Pekov, J. C. Buhl, W. Depmeier, Russian J. Phys. Chem. B 6 (2012) 593-600, DOI: 10.1134/S1990793112050120

[38] D. M. El-Mekkawi, M. M. Selim, J. Environ. Chem. Eng. 2 (2014) 723–730, https://doi.org/10.1016/j.jece.2013.11.014

[39] E. Jordan, R.G. Bell, D. Wilmer, H. Koller, J. Am. Chem. Soc. 128 (2006) 558–567. https://doi-org.lama.univ-amu.fr/10.1021/ja0551887

[40] V. Wernert, R. Denoyel, Mic. Mes. Mat., 222 (2016) 247-255, https://doi.org/10.1016/j.micromeso.2015.10.029

[41] M. Kròl, W. Mozgawa, W. Jastrzebski, J. Porous Mater., 23 (2016) 1-9, DOI 10.1007/s10934-015-0050-6

[42] K. M. Wojciechowsk, M. Kròl, T. Bajda, W. Mozgawa, Materials, 12 (2019), 3271-3289, doi:10.3390/ma12193271

[43] M. Hong, L. Yu, Y. Wang, J. Zhang, Z. Chen, L. Dong, Q. Zan, R. Li, Chem. Eng. J. 359 (2019) 363-372, https://doi.org/10.1016/j.cej.2018.11.087

[44] S. Zhang, M. Cui, J. Chen, Z. Ding, X. Wang, Y. Mu, C. Meng, Materials Letters 236 (2019) 233-235, https://doi.org/10.1016/j.matlet.2018.10.100

[45] M. Miyake, T. Akachi, M. Matsuda, J. Mater. Chem., 15 (2005) 791–79, DOI: 10.1039/b411431k

[46] T. Tügsüz, M. Dogan, F. Sevin, J. Mol. Structure: THEOCHEM 728 (2005) 103–109

List of figures

Figure.1. X-ray diffractograms of a : Agh sample; b : heated clay at 650°C; c: heated at 650°C with NaOH/HC = 4, K: Kaolinite, II: Illite, Qz: quartz, N:Na_2CO_3, * :non identified phase

Figure 2. XRD patterns of the synthesized products obtained at different temperature: (VL) 100°-160°, (L) 160°C-225°C, (M) 225°C-275°C, (H) 275°C-305°C, NaOH/HC=4 (Ther: thermonatrite Na_2CO_3, H_2O)

Figure 3. SEM images of a) Agh, b) Agh treated with NaOH (NaOH/HC=4) and heated at 650°C c) cancrinite zeolite synthesized at high temperature H (275-305°C), NaOH/HC=4

Figure 4. XRD pattern of the synthesized Cancrinite at 130°C-160°C, NaOH/HC=1.2

Figure 5. SEM images of synthesized CAN at 130-160°C, NaOH/HC=1.2

Figure 6. Kinetics of adsorption of Cd^{2+} and Pb^{2+} on clay and synthesized CAN at 298 K

Figure 7. Adsorptions isotherms of a) Cd^{2+} and b) Pb^{2+} on clays and synthesized CAN at 298 K

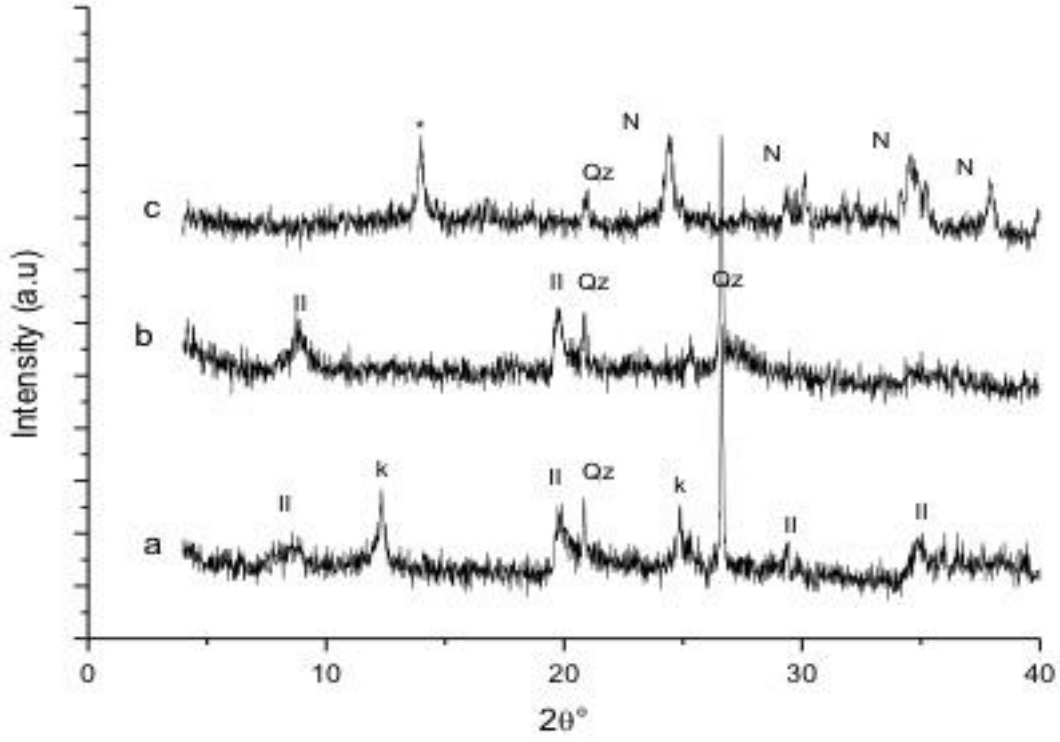

Figure 1.

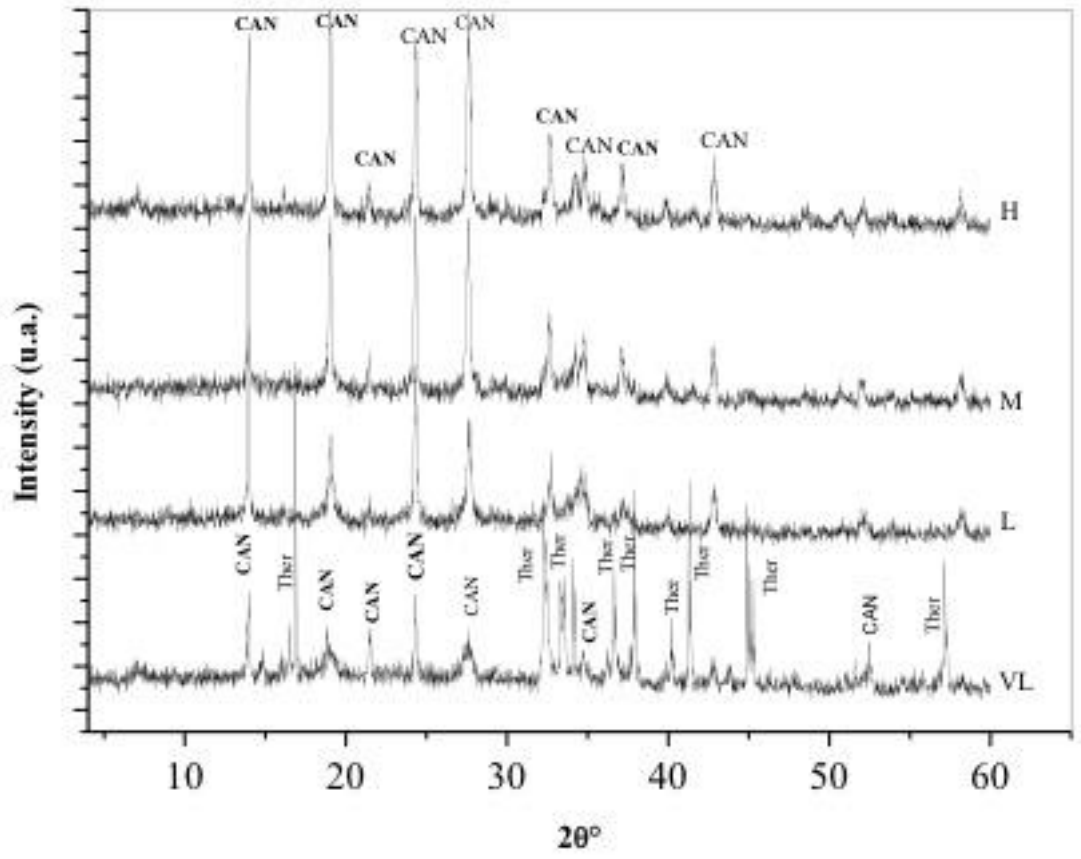

Figure 2.

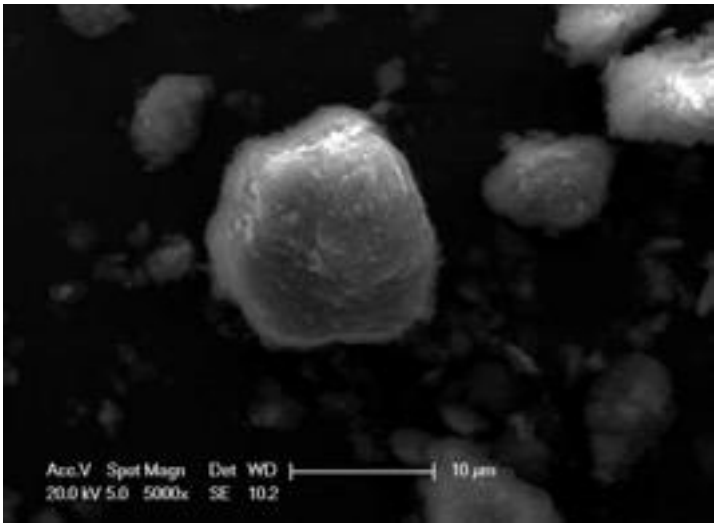

Figure 3a.

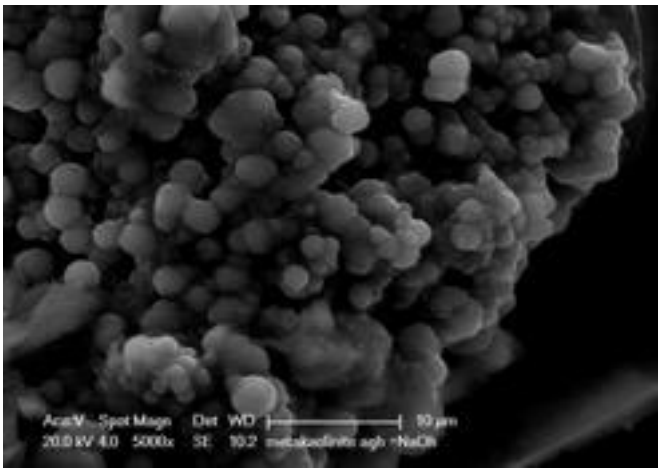

Figure 3b.

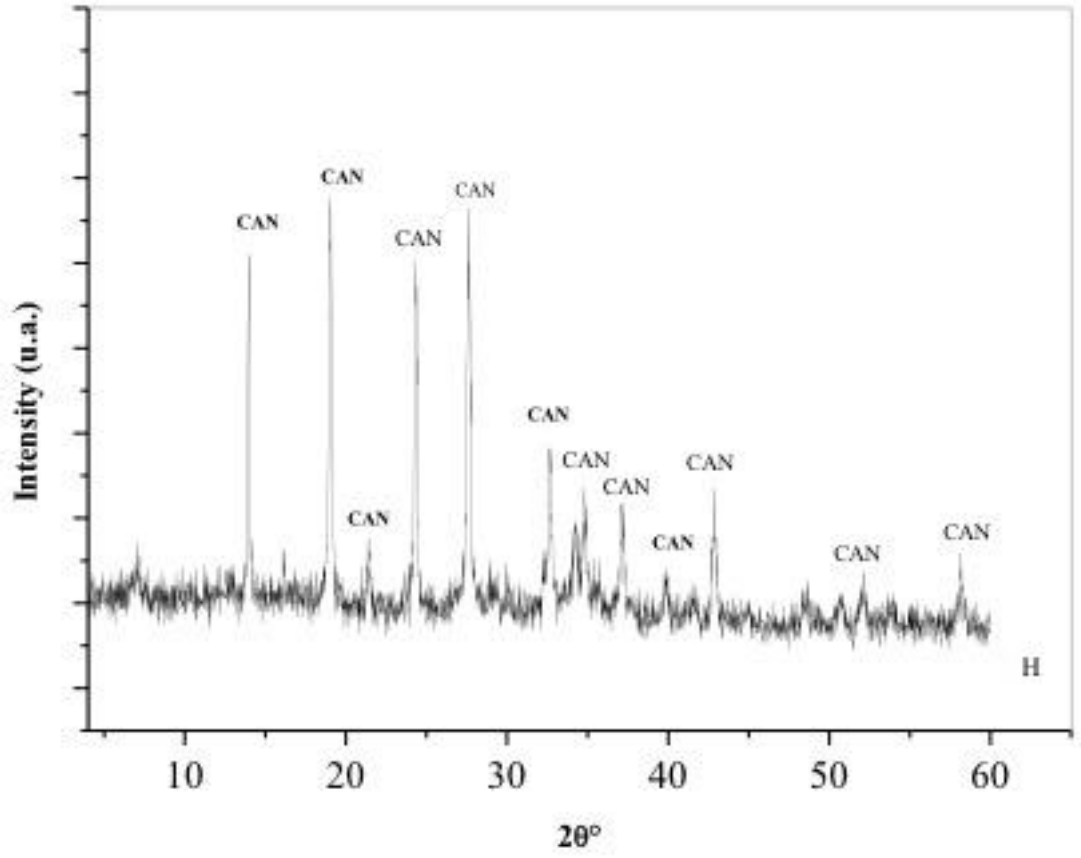

Figure 4.

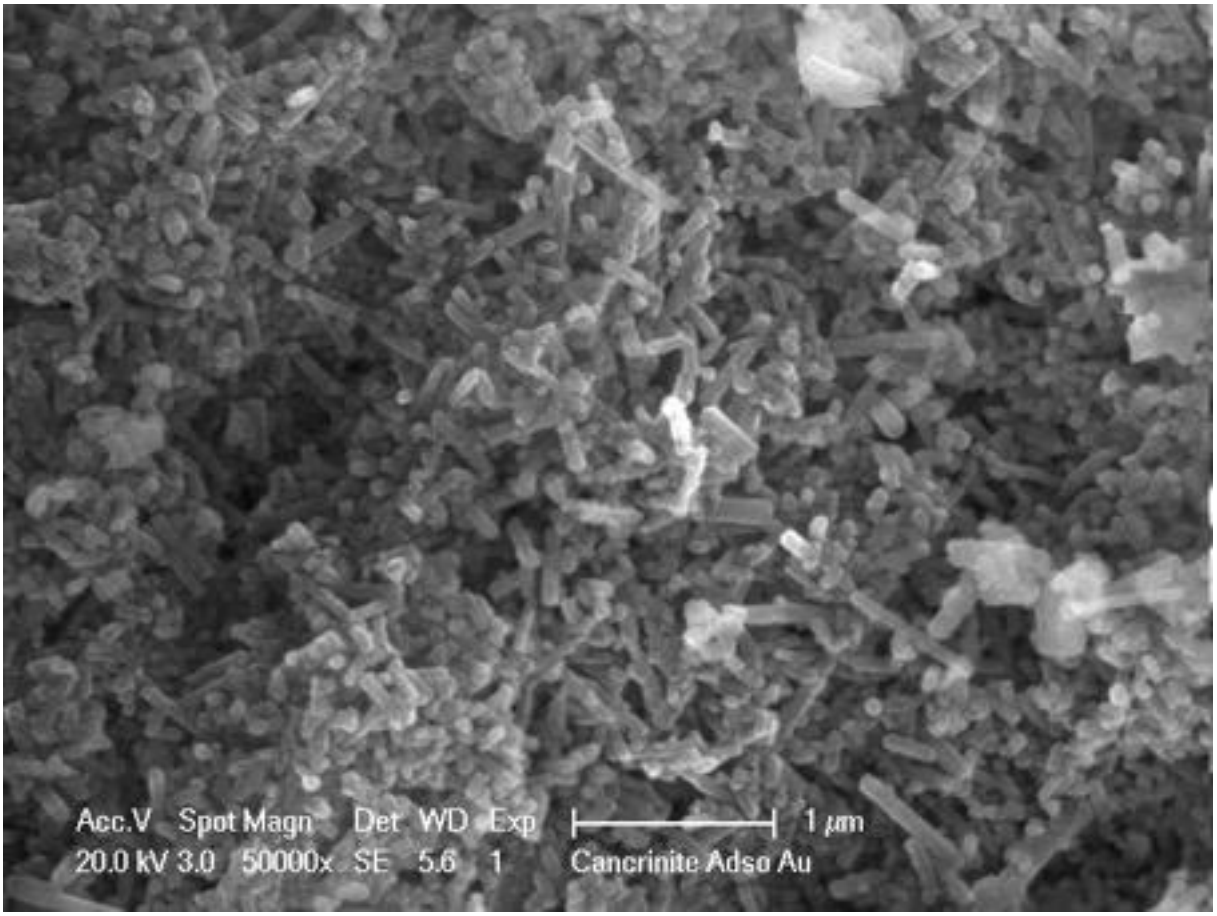
Acc.V Spot Magn Det WD Exp
20.0 kV 3.0 50000x SE 5.6 1
1 µm
Cancrinite Adso Au

Figure 5.

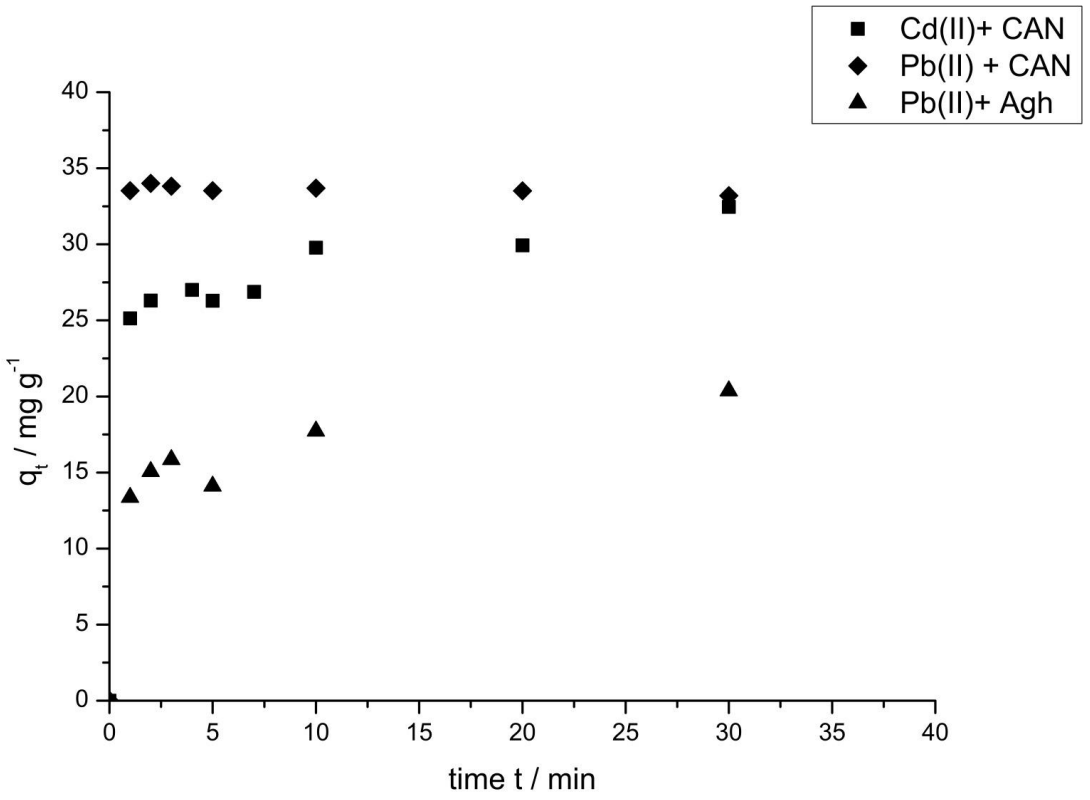

Figure 6.

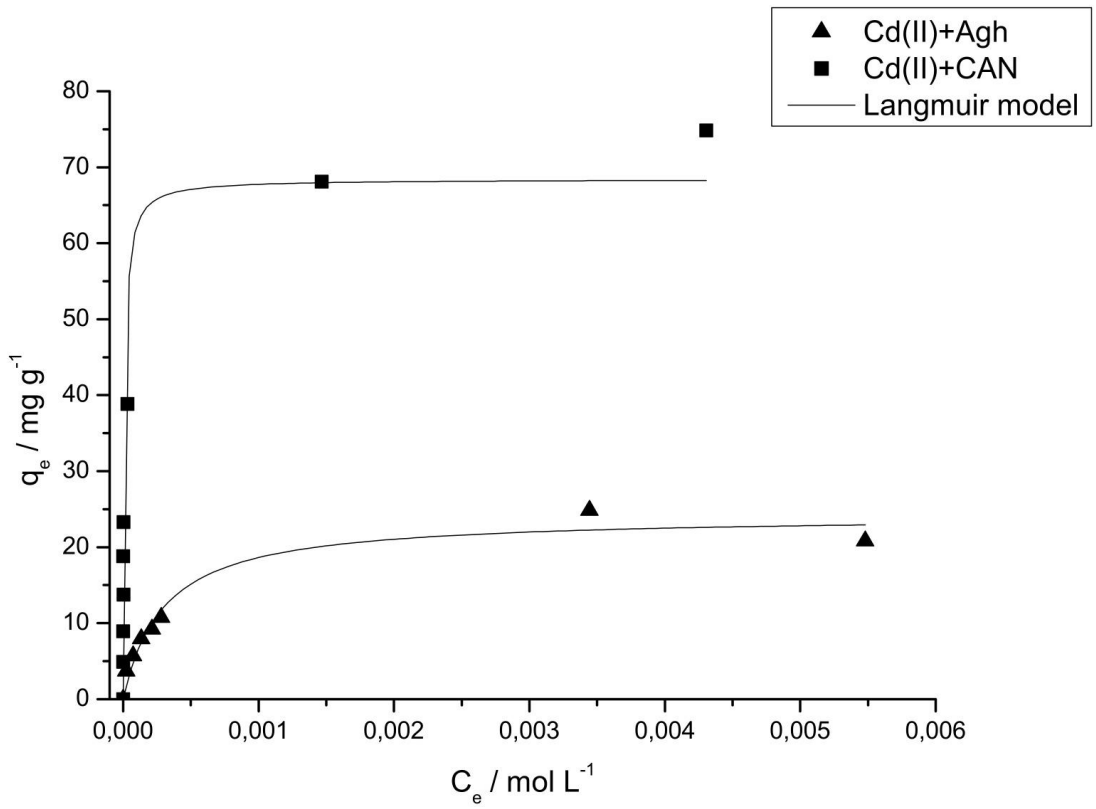

Figure 7a

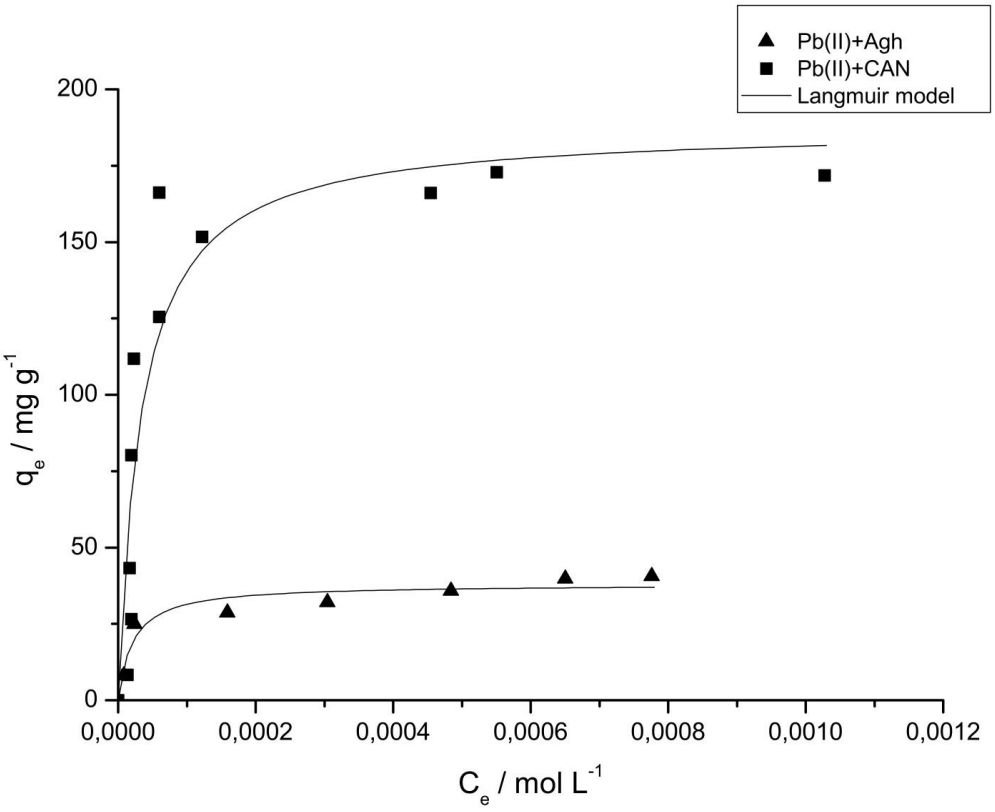
Pb(II)+Agh
Pb(II)+CAN
Langmuir model
200
150
100
50
0
q_e / mg g^{-1}
0,0000
0,0002
0,0004
0,0006
0,0008
0,0010
0,0012
C_e / mol L^{-1}

Figure 7b

List of tables

Table I. Zeolites obtained after hp-hydrothermal synthesis under air and argon for various ratio of NaOH/HC and different temperatures (small containers)

NaOH/HC	Temperature °C	Compounds obtained under air	Compounds obtained under Ar
0.66	85-160	FAU, GIS, CHA* nepheline, Qz	CHA, NAT, GIS, ANA, nepheline, Qz
1	55-170	FAU, GIS, ANA, CAN, SOD, CHA* nepheline, Qz	-
1	170-295	ANA, CAN, GIS, SOD*	-
4	95-160	CAN, thermonatrite	CAN, GIS
4	160-305	pure CAN	CAN, GIS, ANA

ANA: analcime, GIS : gismondine, SOD: sodalite, FAU: faujasite, Qz quartz, *only traces amount

Table II. Zeolites obtained after hp-hydrothermal synthesis under air for various ratio of NaOH/HC and different temperatures (large containers)

NaOH/HC	Temperature °C	Compounds obtained under air
0.66	130-160	ANA
1.2	130-160	CAN, thermonatrite*

* only traces amount

Table III. Thermodynamic parameters for the adsorption of Cd^{2+} and Pb^{2+} onto the different absorbents

Metal	Sample	q_m (mg g^{-1})	K_L*10^{-3} -	$\Delta_{ads}g°$ (kJ mol^{-1})	$\Delta_{ads}h$ (kJ mol^{-1})	$\Delta_{ads}s°$ (J K^{-1} mol^{-1})	$T\Delta_{ads}s°$ (kJ mol^{-1})
Cd^{2+}	Agh	24.2	3.4	-20.1	-0.02	67.4	20.1
	CAN	68.4	100.6	-28.5	5.6	114.7	34.2
Pb^{2+}	Agh	38.0	47.6	-26.7	-	-	-
	CAN	192.6	29.7	-25.5	0.5	87	26.0